ORIGINAL PAPER

New statistical deterministic method for estimating human thermal load and sensation — application in the Carpathian region

Ferenc Ács[1] · Erzsébet Kristóf[1] · Amanda Imola Szabó[1] · Annamária Zsákai[2]

Abstract

A new statistical deterministic model is presented for estimating human thermal load and sensation. Human thermal load is simulated in terms of clothing resistance (r_{cl}) and operative temperature (T_o). The model's input data are wind speed, air temperature, mass of the human body, body length, sex, age, and the latitude of the site. T_o is statistically linked to potential evapotranspiration, whilst human thermal perception to r_{cl}. The model has been validated in the Carpathian Mountains region for the period 1971–2000 comparing it with the original deterministic r_{cl} model. Thermal perceptions of the representative Hungarian male and female are estimated by using individual thermal perception–r_{cl} point clouds. Metabolic heat flux density differences between persons are less than 15 Wm^{-2}. Human thermal perception area distribution has a topography-based configuration. The prevailing annual perception of Hungarians (for both men and women) in lowland and hilly areas is "cool," although "neutral" may also occur; in mountains, perception is mostly "cool" or "cold," with "very cold" being also possible. In the month of July, the perception type in mountains is "neutral" or "cool" depending on the person. In lowland areas, the methodology cannot be applied since the energy balance is not met. The model can also be applied in other heat-deficient regions if the region-specific operative temperature–potential evapotranspiration and the human-specific thermal perception-r_{cl} statistical relationships are determined for the new region.

1 Introduction

Already, von Humboldt (1845) (see also Hantel and Haimberger 2016) observed that all human sensory organs are needed to sense climate, and the sensation will always remain incomplete and it will be subjective. Similarly, human thermal comfort research in the middle of the twentieth century proposed as many as hundreds of factors that determine the outdoor thermal environment (Zhao et al. 2021). This view changed with the appearance of Fanger's work (Fanger 1973). It was Fanger who selected the main environmental and human factors influencing the human thermal environment, which are as follows: air temperature, radiation, wind speed, air humidity, clothing thermal resistance, and activity. Fanger's influence was huge

(Zhao et al. 2021), as he converted the qualitative approach into a quantitative investigation and introduced the energy balance method–based treatment.

In the past decade, energy balance method–based treatments prevailed worldwide (Potchter et al. 2018) and many other methods, such as the device-based methods, algebraic or statistical methods, and methods serving special purposes (de Freitas and Grigorieva 2015), are underrepresented. Note, in this study, de Freitas and Grigorieva's (2015) model type categorization is used. Among energy balance-based methods, physiological equivalent temperature (PET), universal thermal climate index (UTCI), and predicted mean vote (PMV) are the most popular indices. According to Staiger et al. (2019) and Matzarakis (2020), all three indices are suitable for the evaluation of climate from a human biometeorological point of view. Among the three indices mentioned, PET was used most frequently in the Carpathian region (e.g., Gulyás et al. 2006; Gulyás and Matzarakis 2009; Kántor et al. 2012; Bašarin et al. 2014, 2018). In these studies, the climate is analyzed in selected subregions of the Carpathian region.

Studies referring to the whole Carpathian region started to appear from 2020s (Ács et al. 2020a, 2020b).

✉ Ferenc Ács
acs@caesar.elte.hu

[1] Faculty of Science, Institute of Geography and Earth Sciences, Department of Meteorology, Eötvös Loránd University, 1117 Budapest, Hungary

[2] Department of Human Anthropology, Faculty of Science, Eötvös Loránd University, 1117 Budapest, Hungary

In these studies, the human thermal environment is considered in terms of clothing thermal resistance r_{cl} and operative temperature T_o. The scheme is deterministic based on energy balance considerations (de Freitas and Grigorieva 2015). The parameter r_{cl} depends on both T_o and metabolic heat flux density M. T_o expresses the heat load effect, which is triggered by all atmospheric variables (the most important: temperature, radiation, wind, humidity). M refers to a walking human in outdoor conditions whose speed is 1.1 ms^{-1}. The model does not belong to the group of top models according to Staiger et al's (2019) criteria characterizing a model's suitability. In the work of Ács et al. (2021a), mean annual r_{cl} values are statistically interconnected with the annual sum of potential evapotranspiration PE; this is how the first statistical r_{cl} model was constructed. Both r_{cl} and PE depend on the same atmospheric factors (radiation, air temperature, and wind); thus, it can be assumed that the statistical relationship between them might be strong. This was confirmed by Ács et al. (2021a). The analysis showed that r_{cl} results depend also strongly on human body somatotype variations. The model, despite its shortcomings (climate and human-specific), can provide valuable extra human thermal climate information for Thornthwaite-type (Thornthwaite 1948) climate classification models like the Feddema model (Feddema 2005). The study of Ács et al. (2021a) can also be seen as a first attempt to link human and descriptive climate classification methods since generic climate classification models do not include human thermal climate information.

The statistical r_{cl} model of Ács et al. (2021a) can be improved by the statistical interconnection of monthly and annual T_o values and monthly and annual sums of PE. T_o values obtained in such a way can be used for calculating r_{cl} values as in deterministic models (Ács et al. 2020b, 2021b). The benefit of this replacement is twofold: fewer input data are required and the more lengthy and cumbersome calculation of T_o is avoided. The disadvantage is that the statistical interconnection of T_o and PE is climate-specific and limited in space and time. In addition, thermal load expressed in terms of r_{cl} is characterized in terms of thermal sensation. The thermal load–thermal sensation relationship is determined for two individuals by the concurrent collection of weather and thermal sensation data. The thermal sensation–r_{cl} point-cloud is also statistically treated.

According to the above, the aims of this study are as follows: (1) to present this new statistical-deterministic model, (2) to discuss the performance of the model, (3) to discuss individual thermal sensation–r_{cl} relationships, and (4) to characterize the human thermal climate of the Carpathian region in terms of human heat load and thermal sensation on annual, seasonal and monthly time scales. The methods used are described in Section 2. The region and the locations of the cities where the collection of weather data is carried out and the thermal sensation observations are performed are presented in Section 3. The data used in the study are considered in Section 4. The results are presented and described in Section 5, the verification of the results in Section 5.1, the results characterizing the relationship between thermal sensation and thermal load in Section 5.2, and the human thermal climate results in Section 5.3. The suitability of the model is discussed in Section 6. The main conclusions are drawn in Section 7.

2 Methods

Three procedures are used: a scheme for characterizing environmental human thermal load, human thermal sensation observations, and lastly a data treatment method when the statistical link between thermal load and thermal sensation data is handled. Thermal load is characterized in terms of clothing thermal resistance. r_{cl} estimates are made for both weather and climate data. When weather data are used, operative temperature is calculated deterministically (Ács et al. 2020b). In the case of climate data, operative temperature is calculated statistically as presented in the next section.

2.1 Determination of clothing thermal resistance

Clothing thermal resistance is simulated using clothed human body energy balance considerations (Ács et al. 2020b). It can be expressed as

$$r_{cl} = \rho \cdot c_p \cdot \frac{T_S - T_o}{M - \lambda E_{sd} - \lambda E_r - W} - r_{Hr}, \qquad (1)$$

where ρ is air density (kgm^{-3}), c_p is the specific heat at constant pressure (Jkg^{-10} C^{-1}), T_S is the skin temperature (°C), T_o is the operative temperature (°C), M is the metabolic heat flux density (Wm^{-2}), λE_{sd} is the latent heat flux density of dry skin (Wm^{-2}), λE_r is the respiratory latent heat flux density (Wm^{-2}), W is the mechanical work flux density (Wm^{-2}), and r_{Hr} is the combined resistance for expressing the thermal radiative (r_R) and convective (r_{Ha}) heat exchanges (sm^{-1}). These resistance terms can be expressed as

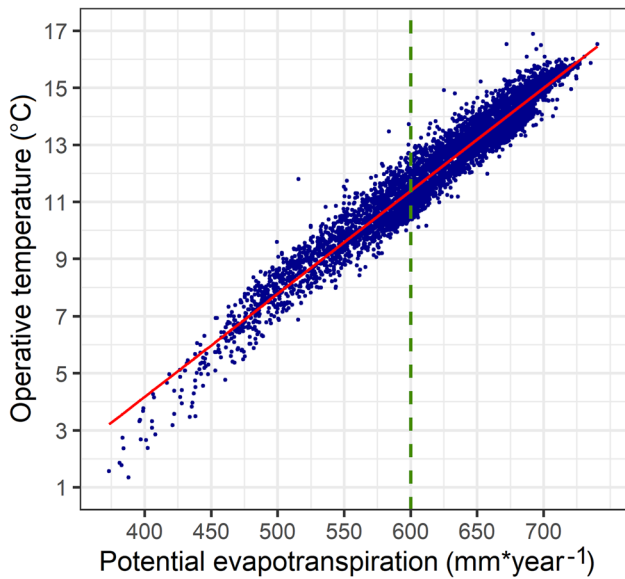$$\frac{1}{r_{Hr}} = \frac{1}{r_{Ha}} + \frac{1}{r_R}, \qquad (2)$$

Fig. 1 Scatter chart of the annual mean of operative temperature as a function of the annual sum of potential evapotranspiration in the CarpatClim dataset region for the period 1971–2000

$$r_{Ha}\left[sm^{-1}\right] = 7.4 \cdot 41 \cdot \sqrt{\frac{D}{U_{1.5}}}, \tag{3}$$

$$\frac{1}{r_R} = \frac{4\epsilon_{cl}\sigma T_a^3}{\rho c_p}, \tag{4}$$

where D (m) is the diameter of the cylindrical body with which the human body is approximated (Campbell and Norman 1998), $U_{1.5}$ is airspeed relative to the human body at 1.5 m, ε_{cl} is the emissivity of clothing or skin (in this study, $\varepsilon_{cl} = 1$), σ is the Stefan-Boltzmann constant, and T_a is the air temperature (°C). $U_{1.5}$ is calculated using wind speed at a height of 10 m and using a logarithmic wind profile supposing neutral thermal stability. As it may be seen, the scheme does not take into account the effect of the direction of a walking human compared to the direction of wind speed.

A human walking at a speed of 1.1 ms^{-1} is considered; the human is not sweating. The human's total metabolic heat flux density is as follows,

$$M = M_b + M_w, \tag{5}$$

where M_b is the basal metabolic rate (W) and M_w is the metabolic rate (W) referring to walking. M_b is parameterized according to Mifflin et al. (1990) separately for men and women

$$M_b^{male}\left[kcal \cdot day^{-1}\right] = 9.99 \cdot M_{bo} + 6.25 \cdot L_{bo} - 4.92 \cdot age + 5, \tag{6}$$

$$M_b^{female}\left[kcal \cdot day^{-1}\right] = 9.99 \cdot M_{bo} + 6.25 \cdot L_{bo} - 4.92 \cdot age - 161, \tag{7}$$

where M_{bo} is body mass (kg), L_{bo} is body length (cm), and *age* is expressed in years. The human body surface A (m^2) has to be estimated in order to express M_b in Wm^{-2}, and for this, we use the well-known Dubois and Dubois (1915) formula,

$$A = 0.2 \cdot M_{bo}^{0.425} \cdot \left(\frac{L_{bo}}{100}\right)^{0.725}. \tag{8}$$

M_w is parameterized according to Weyand et al. (2010) as follows,

$$M_w = 1.1 \cdot \frac{3.80 \cdot M_{bo} \cdot \left(\frac{L_{bo}}{100}\right)^{-0.95}}{A}. \tag{9}$$

The coefficient 1.1 is added because of the chosen walking speed. The $\lambda E_{sd} + \lambda E_r$ sum can be expressed as a percent of M (Campbell and Norman 1998), whilst W is parameterized according to Auliciems and Kalma (1979).

2.1.1 Estimation of operative temperature

Operative temperature is statistically evaluated using regression curves obtained by the statistical interconnection of T_o and PE on annual and monthly time scales. The regression curve equations refer to the CarpatClim dataset region for the period 1971–2000. Monthly estimates are performed only for vegetation period months from April to September. The equations linking T_o and PE are as follows,

Year

$$T_o^{annual} = 0.03608 \cdot PE^{annual} - 10.26. \tag{10}$$

Vegetation period months

$$T_o^{April} = 0.0001 \cdot PE_{April}^3 - 0.0092 \cdot PE_{April}^2 + 0.4179 \cdot PE_{April} + 0.6810, \tag{11}$$

$$T_o^{May} = 0.0001 \cdot PE_{May}^3 - 0.0223 \cdot PE_{May}^2 + 2.1093 \cdot PE_{May} - 54.3862, \tag{12}$$

$$T_o^{June} = 0.0001 \cdot PE_{June}^3 - 0.0459 \cdot PE_{June}^2 + 5.3414 \cdot PE_{June} - 190.6055, \tag{13}$$

$$T_o^{July} = 0.0001 \cdot PE_{July}^3 - 0.0472 \cdot PE_{July}^2 + 6.1240 \cdot PE_{July} - 246.8911, \tag{14}$$

$$T_o^{August} = 0.0002 \cdot PE_{August}^3 - 0.0737 \cdot PE_{August}^2 + 8.5701 \cdot PE_{August} - 315.4450, \tag{15}$$

$$T_o^{September} = 0.0002 \cdot PE_{September}^3 - 0.0358 \cdot PE_{September}^2 \\ + 3.2006 \cdot PE_{September} - 82.9106. \quad (16)$$

Both indicators express thermal load; T_o is prevalent in human biometeorology, whilst PE is frequently used in environmental and hydrological surveys. Both T_o and PE depend upon the same meteorological variables; therefore, the statistical relationship between them is strong.

The T_o–PE point clouds together with regression curves for the year and for the month of July are presented in Figs. 1 and 2, respectively. As it can be seen, a linear and a third-order polynomial fitting is used linking T_o and PE.

2.1.2 Calculation of potential evapotranspiration

PE is calculated in the simplest way using only T_a and daylight length as inputs (McKenney and Rosenberg 1993). For the ith month ($i = 1, …, 12$)
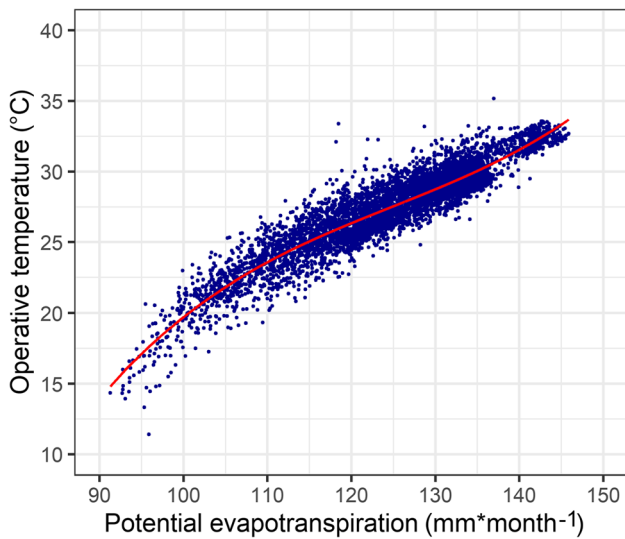

Fig. 2 Scatter chart of the July mean of operative temperature as a function of the July sum of potential temperature in the CarpatClim dataset region for the period 1971–2000

$$PE_i = 1.6 \cdot \left(\frac{L_i}{12}\right) \cdot \left(\frac{N_i}{30}\right) \cdot \left(\frac{10 \cdot T_{ai}}{I}\right)^A, \quad (17)$$

where I is a heat index introduced by Thornthwaite (1948) as

$$I = \sum_{i=1}^{12} t_i, \quad (18)$$

$$t_i = \begin{cases} \left(\frac{T_{ai}}{5}\right)^{1.514}, & \text{if } T_{ai} > 0 \\ 0, & \text{if } T_{ai} \leq 0, \end{cases} \quad (19)$$

$$A = 6.75 \cdot 10^{-7} \cdot I^3 - 7.71 \cdot 10^{-5} \cdot I^2 + 1.792 \cdot 10^{-2} \cdot I + 0.49239. \quad (20)$$

N_i is the number of days in the ith month, T_{ai} is the mean monthly air temperature [°C] of the ith month, and L_i is the mean monthly daylight length [hours]. In our calculations, L_i is estimated by calculating L_i for the central day of the month (the 15th day in the month except for February) as follows,

$$L_i = \frac{24}{180} \cdot \arccos\left[-tg(\varphi) \cdot tg(\delta_i)\right] \quad (21)$$

where φ is latitude [°] and δ_i is declination [°] on the central day of the ith month.

2.2 Determination of thermal sensation

Two individuals, a male and a female (their human state variables are presented in Table 1, see Section 4.3) served as the tools for the qualitative estimation of thermal state performing thermal sensation observations. Both individuals were asked to use the following thermal sensation type groups: very cold, cold, cool, neutral, slightly warm, warm, and very warm. Both persons are native in the region of the Hungarian lowland, where the climate can be characterized either as *Cfb* (*C*, warm temperate; *f*, no seasonality in the annual course of precipitation; *b*, warm summer) according to Köppen (1936), or as "cool and dry with extreme variations of temperature" according to Feddema (2005). During thermal sensing (usually lasting a minimum of 5 min),

Table 1 Human state variables and metabolic heat flux densities of four persons (person 1, a male; person 2, a female; person 3, a representative Hungarian male; person 4, a representative Hungarian female)

Persons	Sex	Age [years]	Body mass [kg]	Body length [cm]	Basal metabolic heat flux density [Wm^{-2}]	Walking energy flux density [Wm^{-2}]	Total energy flux density [Wm^{-2}]
Person 1	Male	64	89.0	190.0	40.8	94.5	135.3
Person 2	Female	34	64.5	160.5	38.6	103.9	142.5
Person 3	Male	19	85.5	179	45.2	101.7	146.9
Person 4	Female	33	65.5	169	38.8	96.1	134.9

sweating or shivering did not occur and, of course, the observers were not aware of their vasodilation or vaso-constriction processes, not to mention other hidden ther-moregulatory processes.

## 2.3 Thermal sensation and thermal load data treatment

Weather and thermal sensation data are collected concur-rently, and the collected data then being filtered. First, the consistency between thermal load and thermal sen-sation data was checked. All those observations were removed where (a) positive clothing thermal resistance values were associated with the thermal sensation types "slightly warm" or "warm" and (b) negative clothing thermal resistance values were found. In the latter cases, the energy balance of the human body covered with clothing is not met because the sweating process is not simulated. Second, each thermal sensation group below the 5th and above the 95th percentiles of the associated T_o values was omitted. As mentioned, T_o is calculated

deterministically (Ács et al. 2020b) taking into account all relevant weather elements (air temperature, radiation, wind speed, air humidity).

3 Region and locations

The CarpatClim dataset region is the region studied. The region together with the locations of the cities where the collection of weather and thermal sensation data is per-formed is presented in Fig. 3. This Central East Euro-pean region is bounded by the 17° and 27°/44° and 50° longitude/latitude lines. It contains both lowlands and mountain areas with quite different climate types rang-ing either from *Cfa* (*C*, warm temperate; *f*, no seasonality in the annual course of precipitation; *a*, hot summer) to ET (tundra climate) according to Köppen (1936) or from "cool and dry with extreme variations of temperature" to "cold and saturated with medium variations of tempera-ture and precipitation" according to Feddema (2005). The cities are located in the lowland region.

Fig. 3 The region of the CarpatClim dataset and the locations (in red) of the cities where the collection of weather data is carried out and the thermal sensation observations are performed. The picture also contains basic elevation data and major geographical desig-nations used in the study
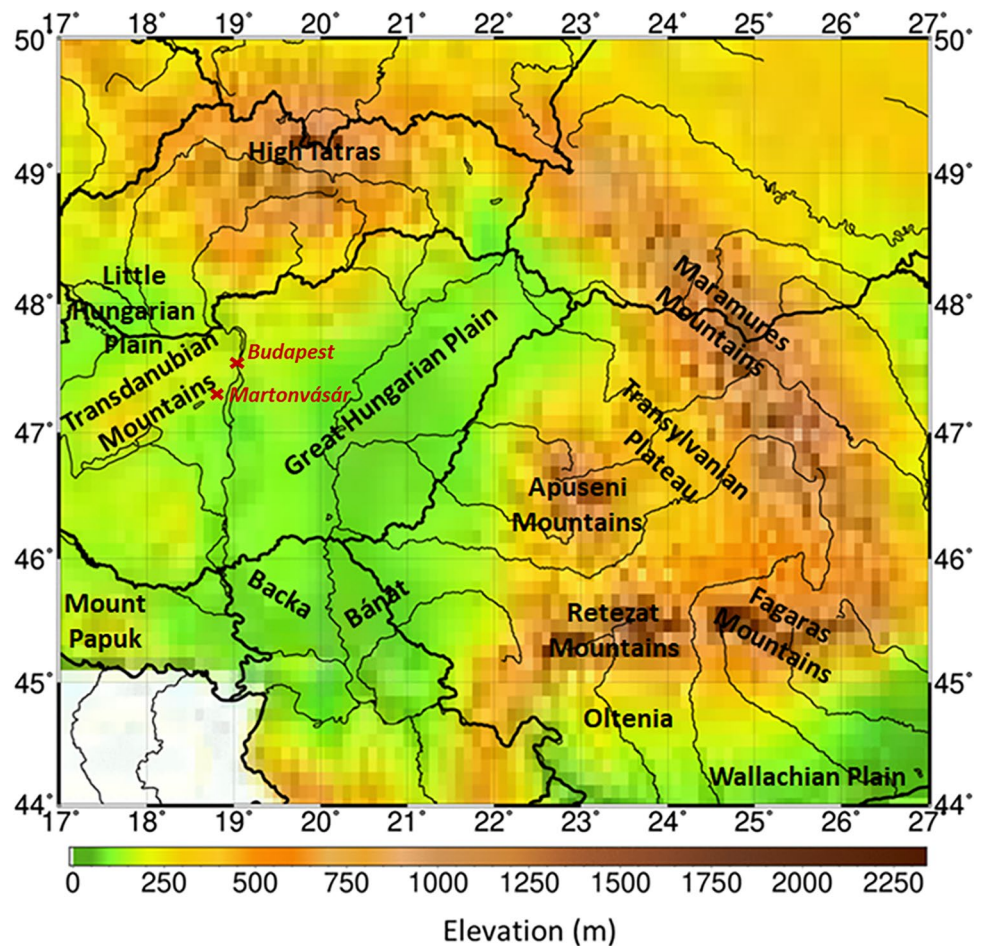
4 Data

Three types of data are used: climatic, weather, and human data. The main characteristics of each data type are separately considered.

4.1 Climatic data

Climatic data are taken from the CarpatClim dataset (Lakatos et al. 2013). The dataset is based on station observations. The number of stations taken into account depends upon the type of climatic element; it can vary between 300 and 1000 (Cheval et al. 2014). Among climatic data, we used the following: daily values of air temperature and wind speed at a height of 10 m. Daily data are quality controlled and homogenized by using the MASH (Multiple Analysis of Series for Homogenization) procedure (Szentimrey 1999). Monthly values are constructed from the daily values. The 30-year mean monthly values are calculated for the period 1971–2000. The spatial resolution of the data is $0.1° \times 0.1°$, which is equivalent to about 10 km × 10 km. Interpolation and gridding procedures are performed by using the MISH (meteorological interpolation based on surface homogenized data basis) method (Szentimrey and Bihari 2013).

4.2 Weather data

Weather data in cities are taken from the nearest automatic meteorological station operated either by the Hungarian Meteorological Service (HMS) or by a private company "Időkép." The beeline distance between the automatic stations and the thermal sensation observation locations was in both cases shorter than 3 km. Air temperature, air humidity, wind speed, and atmospheric pressure are used from the measured data. Relative sunshine duration and cloudiness are estimated by observers.

Person 1 collected weather data in the period April 1, 2020–February 20, 2021. Observations are performed in the day and night as well under a large variety of weather conditions. In night-time periods (about 40% of the cases), air temperature ranged between −11 and 28 °C, mostly still wind conditions prevailed, but there were also high average wind speeds of 4 and 7 ms^{-1}. Relative air humidity varied between 40 and 100%. In daytime periods, global radiation and air temperature varied between 10 and 850 Wm^{-2} and between −9 and 32 °C, respectively. Wind was in most cases moderate, between 2 and 3 ms^{-1}, but, of course, there were also higher (average wind speed about 6–7 ms^{-1}, gusts above 10 ms^{-1}) and lower (under 1 ms^{-1}) wind speed values. Relative air humidity varied between 20 and 100%.

Person 2 collected weather data in the period April 7, 2020–March 2, 2021. About two-thirds of the observations were carried out in anticyclonic weather conditions. The air pressure values vary between 993 and 1038 hPa. There was no precipitation at the time of the observations. In night-time periods (about 35% of the cases), the air temperature ranged between −10 and 23 °C, while relative humidity varied between 40 and 100%. The average wind speed ranged between 0.1 and 6.7 ms^{-1}. In daytime periods, air temperature values varied between −9 and 34 °C while the relative humidity values were between 15 and 100%. The average wind speed varied from calm (0.1 ms^{-1}) to high values (7.8 ms^{-1}).

4.3 Human data

The human state variables used are as follows: body mass (the most important), body length, sex, and age. These personal data of four individuals together with calculated metabolic heat flux densities are presented in Table 1.

Data of persons 1 and 2 are used for determining the relationship between thermal sensation and thermal load. Metabolic heat flux densities of persons 3 and 4 are as close as possible to the metabolic heat flux densities of a representative Hungarian male and female, respectively (Zsákai et al. 2015; Bodzsár et al. 2016).

5 Results

Three result types are considered: (1) verification results, (2) thermal sensation–thermal load relationship results, and (3) results characterizing the human thermal climate of the region considered.

5.1 Verification results

Verification results are constructed for persons 3 and 4 since their total energy flux densities are as close as possible to the total energy flux densities of an average Hungarian male and female, respectively. Figure 4 shows scatter plots between clothing thermal resistance values obtained by calculating operative temperature as a function of PE (statistical deterministic model) and by calculating operative temperature according to its definition (e.g., Ács et al. 2021b) (deterministic model).

The figure contains 4 scatter plots: for person 3 (representative Hungarian male) for the year and the month of July and the same for person 4 (representative Hungarian female). Straight lines at 45° are also plotted. It can be said that the agreement is good, especially for the year. For the annual estimate, there is a slight underestimation

Fig. 4 Comparison of clothing thermal resistances obtained by calculating operative temperature by using statistical deterministic and deterministic procedures for a representative Hungarian male and female in the month of July (top) and in the year (bottom) in the CarpatClim dataset region for the period 1971–2000. Each point cloud contains a few thousand points
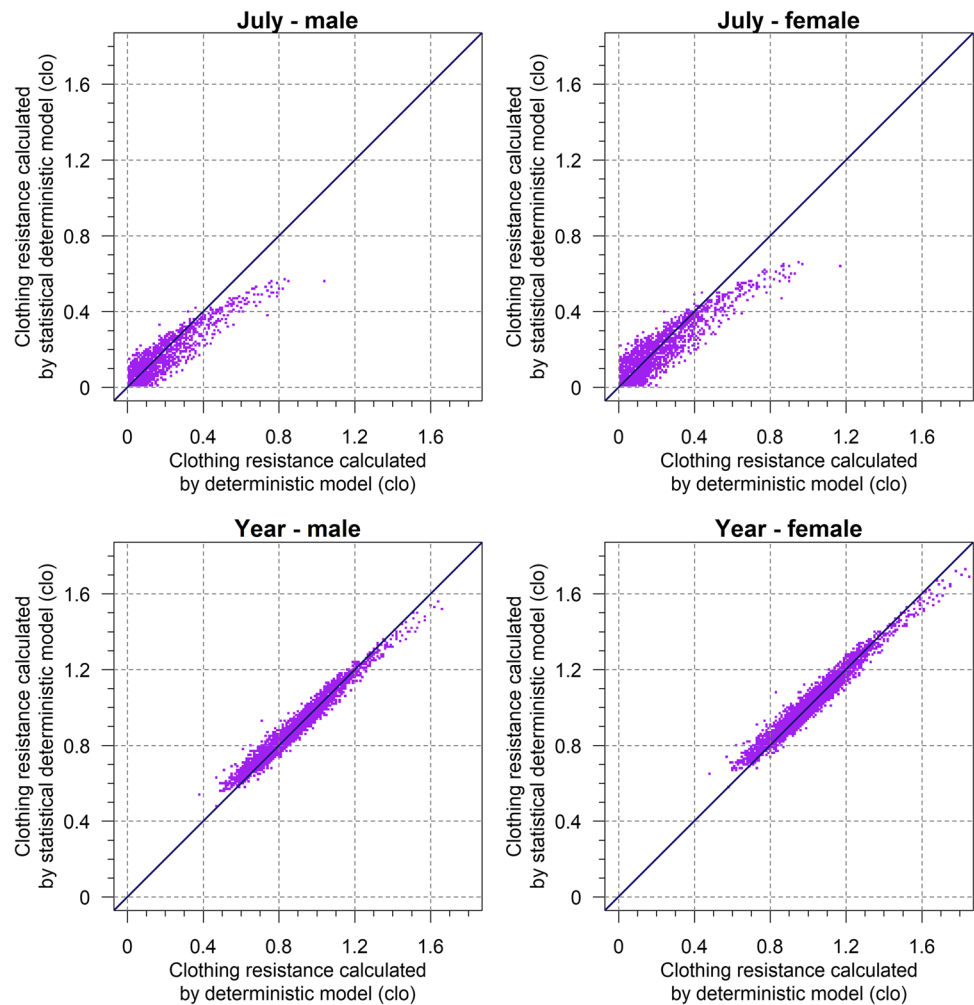
in the zones of higher r_{cl} values (r_{cl} is higher than 1.3 (clo), such cases are obviously in the mountainous areas). A similar underestimation in the zone of higher r_{cl} values (r_{cl} is higher than 0.3–0.4 (clo)) also exists for the month of July. This underestimation is somewhat larger as for the annual period. Note that the characteristics of the agreement are equally valid for male and female.

The agreement in terms of area distribution for the representative Hungarian male and female is presented in Figs. 5 and 6, respectively.

As we might have expected from Fig. 4, noticeable differences can be found only in mountainous areas, for example, in the Apuseni Mountains, Retezat Mountains, and Fagaras Mountains. The agreement in lowland areas is more noticeable than the agreement in mountainous areas.

## 5.2 Individual thermal sensation–thermal load relationships

Thermal sensation–thermal load relationships are determined for persons 1 and 2. Thermal load is expressed in terms of clothing thermal resistance. Note that the total energy flux densities of persons 1 and 2 are in the range of the total energy flux densities of persons 3 and 4, who represent the representative Hungarian male and female. These relationships are presented in Fig. 7.

Person 1 is represented by triangles, whilst person 2 by circles. The r_{cl} ranges registered for the thermal sensation categories used can be seen in Table 2.

There are 236 and 242 points in total for persons 1 and 2, respectively. Each point represents a weather situation. Examining Figs. 7 and Table 2, two facts can be established: (1) the smallest inter-person deviations in r_{cl} values are obtained for the thermal sensation types "neutral" and "cool." The inter-person deviations in r_{cl} values increase towards cold stresses. In our case, the largest deviations appeared in the thermal sensation category "very cold." (2) In this case, discrete thermal sensation categories are used, at the same time, human thermal perception is continuous, and it is hard to separate it into different discrete types. Therefore, the adjacent thermal categories are not unequivocally separated by r_{cl} values;

Fig. 5 Area distribution of annual clothing resistance values obtained by calculating operative temperature by using deterministic (top, (**a**)) and by statistical deterministic (bottom, (**b**)) procedures for a representative Hungarian male in the CarpatClim dataset region for the period 1971–2000
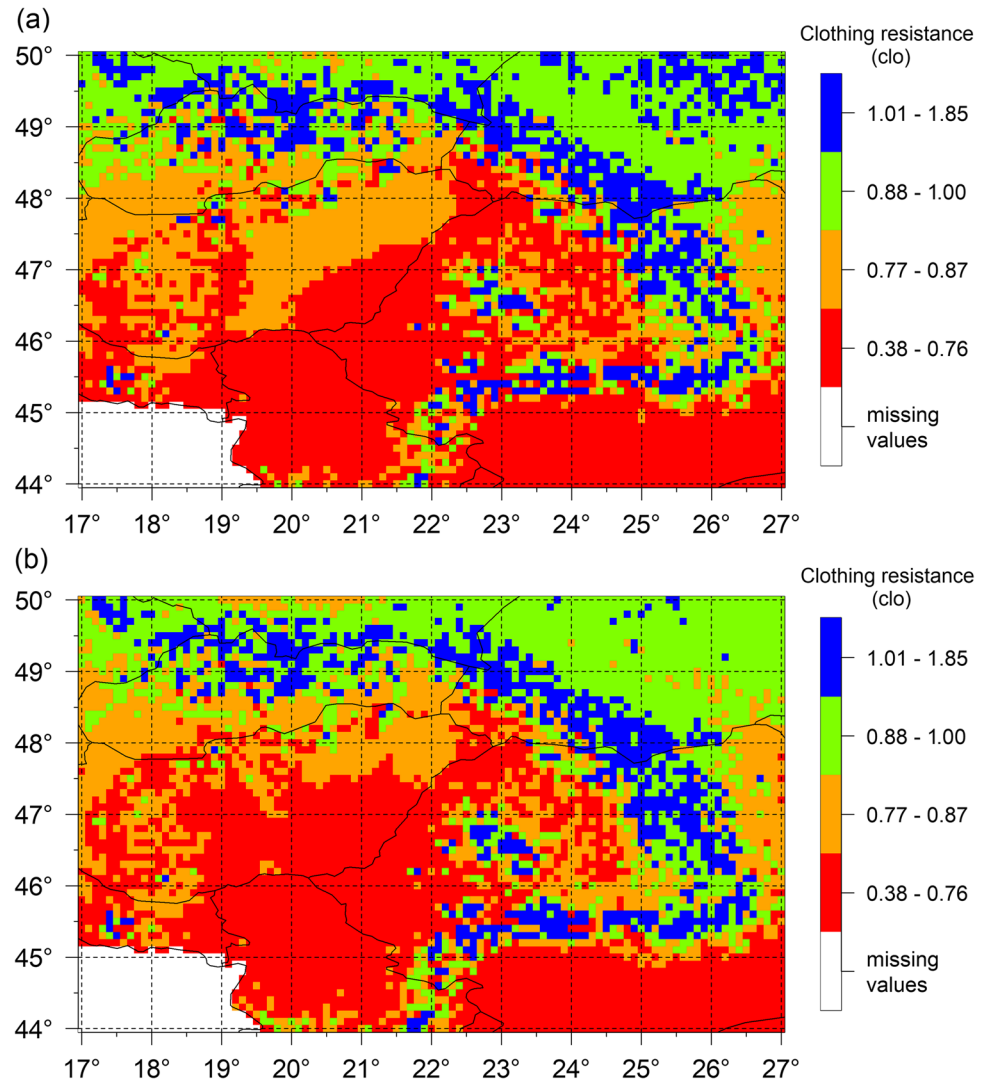
5.3 Human thermal climate

Human thermal climate characteristics will be separately considered for the time periods, year, the month of July, and for the vegetation period from April to September.

5.3.1 Year

Annual area distributions of clothing thermal resistance for the representative Hungarian male and female are presented in Figs. 5b and 6b, respectively. Both area distribution structures follow the area distribution structure of topography. The lowest r_{cl} values (in red) are in southern lowland regions (Backa, Banat,

Oltenia, Wallachian Plain). The r_{cl} values in the Great Hungarian Plain are slightly larger with respect to the former lowland regions. In the hilly and foothills regions (e.g., Transdanubian Mountains, Transylvanian Plateau, eastern foothills of Carpathians), r_{cl} values can even reach 1 (clo) (in green). The largest r_{cl} values can be found in mountain regions, like Retezat, Fagaras, the Maramures Mountains, and the High Tatras. In these areas, r_{cl} can vary between 1 and 1.8 (clo). Note that area distribution structures for male and female are very similar, although there is a slight shift between their r_{cl} values. This is logical because their M values are different.

These thermal loads are perceived by humans 1 and 2 together as follows: a thermal load of 0.4–0.8 (clo) (in red) is perceived mostly as "neutral" or "cool," but the perception "cold" may also occur, especially for persons whose M is lower than 135 Wm^{-2}. For a slightly larger thermal load of 0.7–1.0 (clo) (in orange and green), only

Fig. 6 Area distribution of annual clothing resistance values obtained by calculating operative temperature by using deterministic (top, (**a**)) and by statistical deterministic (bottom, (**b**)) procedures for a representative Hungarian female in the CarpatClim dataset region for the period 1971–2000
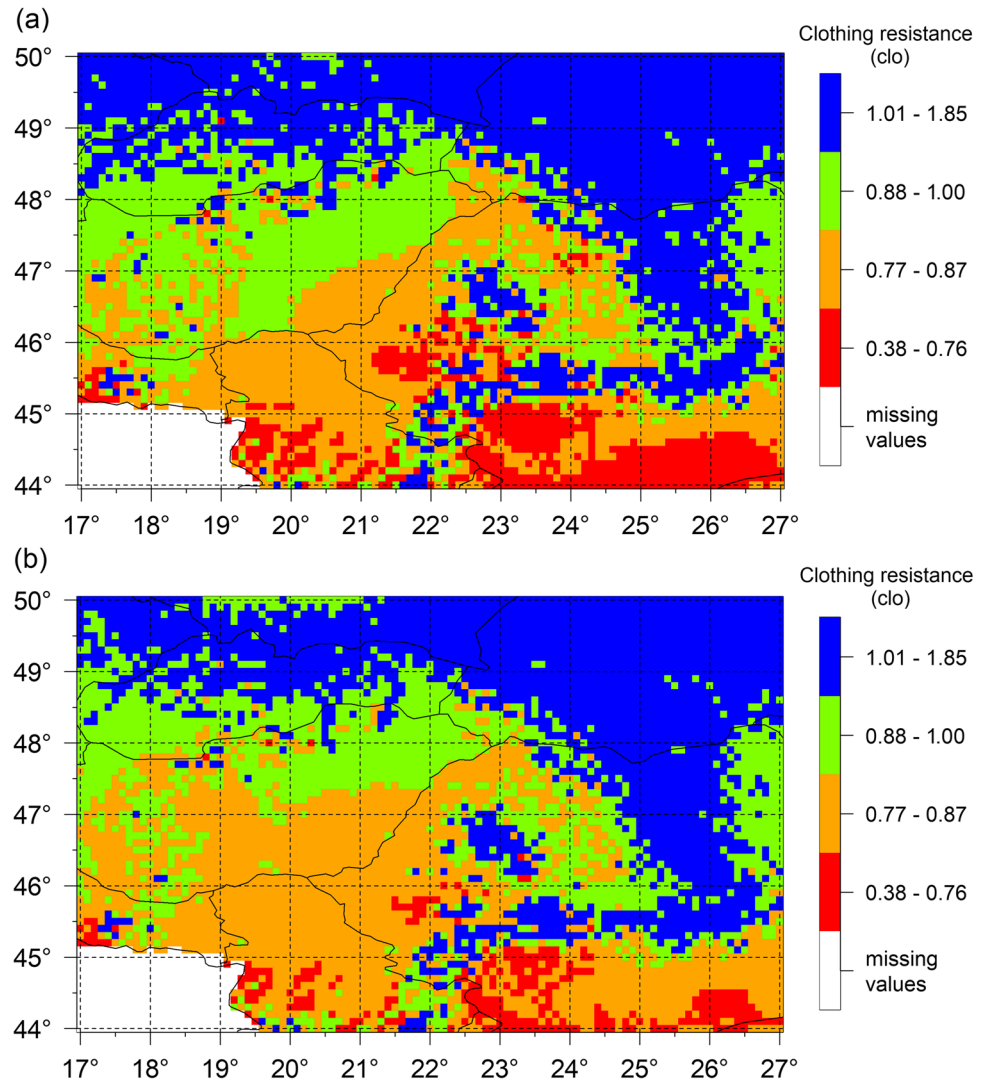
the perceptions "cool" and "cold" occur; of course, this depends on the person and their psychological state, which perception is represented to a greater extent. A thermal load of 1–1.8 (clo) (in blue) can be sensed as "cool," "cold," or "very cold." Note that in these areas, the importance of personal differences on the evolution of thermal perception is much higher than in lowland and hilly regions. This means that in mountain regions, the same thermal load can be sensed either as "cool" or as "very cold" depending on the person and their psychological state.

5.3.2 July

The area distributions of clothing thermal resistance for the month of July for the representative Hungarian male and female are presented in Figs. 8 and 9, respectively.

In the month of July, the method is applicable only in mountain areas. In the mountains, r_{cl} values can vary

between 0 and 1.2 (clo). This thermal load is perceived by humans 1 and 2 as "neutral" or "cool." As mentioned, the method is not applicable in lowland and hilly areas. Nevertheless, we can state that in these areas, the most common thermal perception types are "neutral" and "slightly warm." Thus, in the month of July, the thermal perception type "neutral" is common in the Carpathian Basin.

5.3.3 The vegetation period from April to September

The area distributions of clothing thermal resistance for the 6-month period from April to September (hereinafter vegetation period) for a representative Hungarian male and female are presented in Figs. 10 and 11, respectively.

As in the previous case, the method is applicable only in mountain areas. r_{cl} values can vary between 0 and 1.2 (clo), but very low (0–0.2 (clo)) r_{cl} values are predominant. This is sensed as "neutral" by humans 1 and 2, but in higher areas, thermal perception types "cool"

Fig. 7 The thermal sensation–clothing thermal resistance relationships for persons 1 and 2
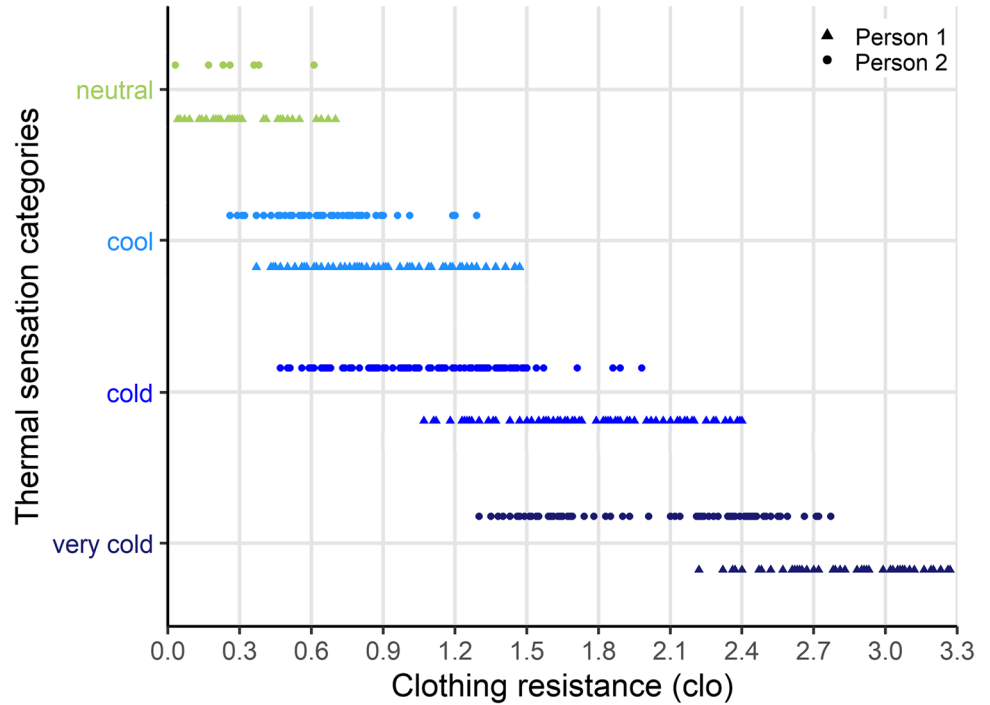

Table 2 Clothing resistance ranges of persons 1 and 2 for different thermal sensation categories

Thermal sensation category	Clothing thermal resistance (r_{cl}) range of person 1 (clo)	Clothing thermal resistance (r_{cl}) range of person 2 (clo)
Neutral	$0 < r_{cl} < 0.7$	$0 < r_{cl} < 0.6$
Cool	$0.4 < r_{cl} < 1.5$	$0.3 < r_{cl} < 1.3$
Cold	$1.1 < r_{cl} < 2.4$	$0.4 < r_{cl} < 1.7$
Very cold	$2.2 < r_{cl} < 3.3$	$1.3 < r_{cl} < 2.8$

and "cold" may also occur. Area distributions obtained for man and woman are very similar, but the differences increase with increasing altitude. As mentioned, the method is not applicable in lowland and hilly areas. Note that the applicability of the method for man and woman differs unequivocally in the Podolian upland (top right corner in the figures). Note how common is the thermal perception type "neutral" in the mountains during the vegetation period.

Fig. 8 Area distribution of July clothing thermal resistance values obtained by calculating operative temperature by using the statistical deterministic procedure for a representative Hungarian male in the CarpatClim dataset region for the period 1971–2000
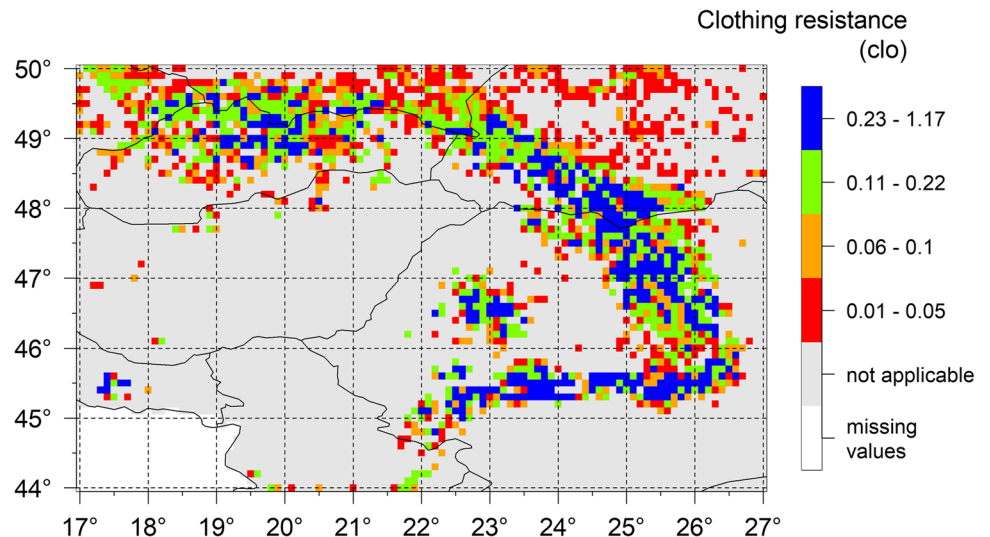
Fig. 9 Area distribution of July clothing thermal resistance values obtained by calculating operative temperature by using a statistical deterministic procedure for a representative Hungarian female in the CarpatClim dataset region for the period 1971–2000
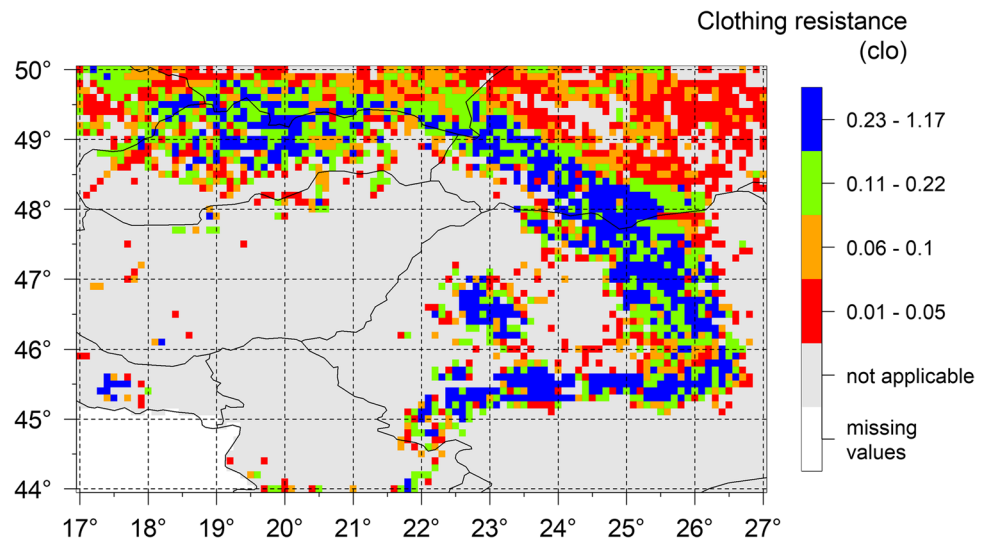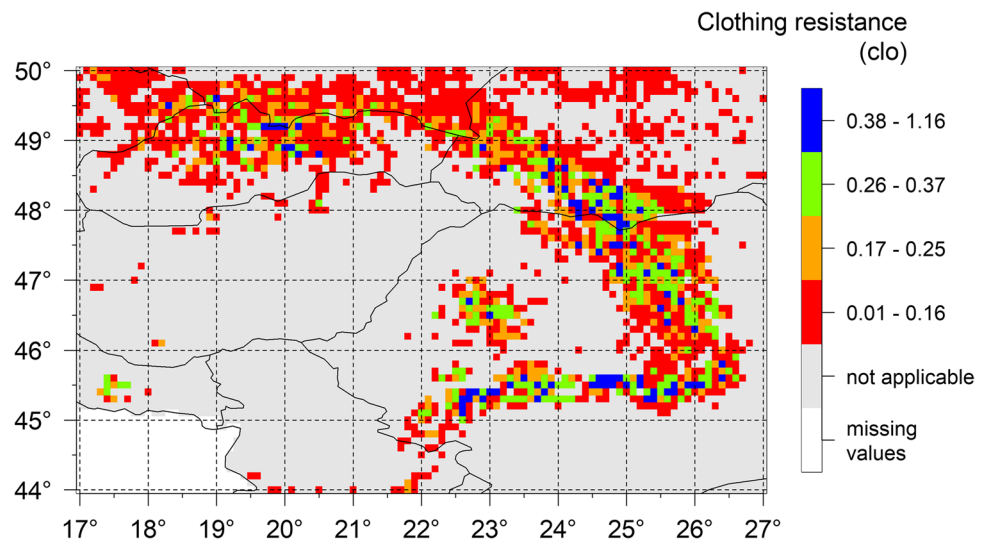

Fig. 10 Area distribution of vegetation period clothing thermal resistance values obtained by calculating operative temperature by using the statistical deterministic procedure for a representative Hungarian male in the CarpatClim dataset region for the period 1971–2000

Fig. 11 Area distribution of vegetation period clothing thermal resistance values obtained by calculating operative temperature by using the statistical deterministic procedure for a representative Hungarian female in the CarpatClim dataset region for the period 1971–2000
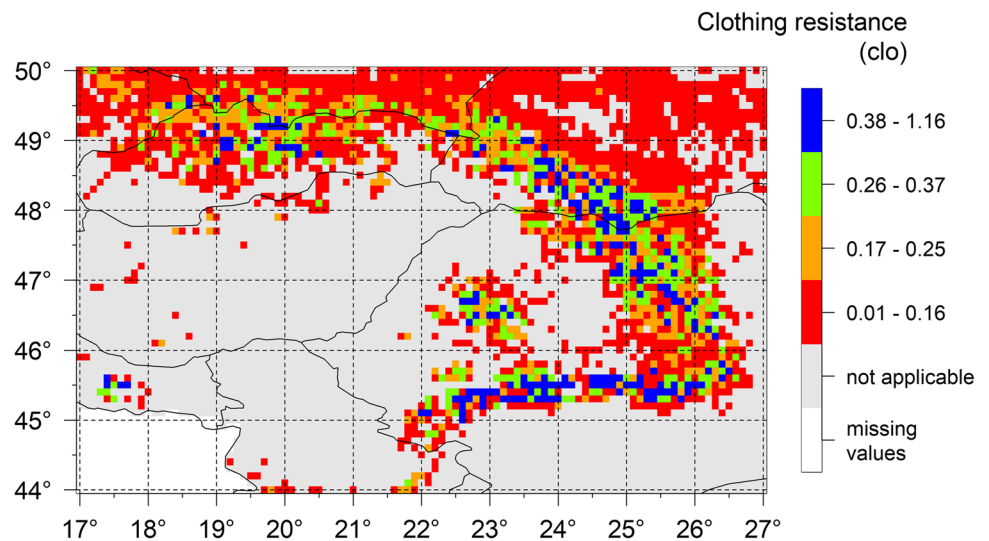
6 Discussion

So far, mainly complex, energy balance–based models have been used for estimating human thermal load (e.g., Gagge et al. 1986; Mayer and Höppe 1987; Staiger et al. 2012; Jendritzky et al. 2012; Fiala et al. 2011; Blazejczyk et al. 2012). These types of models (mostly PET and UTCI models) have also been applied to the Carpathian Basin (e.g., Németh 2011; Kovács and Németh 2012; Kovács and Unger 2013). Most recently, human thermal load estimations in the Carpathian region are also made by applying a clothing index model (e.g., Ács et al. 2020a, 2020b). The PET, the UTCI, and the clothing index models are energy balance–based models (de Freitas and Grigorieva 2015), but they differ enormously in terms of model type and results. In such cases, it is especially difficult to compare and interpret the obtained results (Potchter et al. 2022). Regarding the model types, we can briefly say the following: PET and UTCI are working in a "forward mode"; that is, the skin temperature or clothing's surface temperature is the variable to be calculated. The clothing index model is working in "backward mode"; that is, the skin temperature is known, and the thermal resistance of the clothing is the variable to be calculated. As a consequence of this difference in model structure, the clothing index model is much simpler than the UTCI or PET model. The clothing index model is an inverse Fanger model (Fanger 1970) analyzing a single-segment human body (Enescu 2019). The UTCI model contains 12 segments and 187 nodes, whilst PET has 1 segment and 2 nodes. The most popular model is PET. The UTCI applications are also not rare, but the clothing index models are the most rarely used ones. The UTCI and PET models can be successfully applied in both warm and cold climates. The clothing index model can only be successfully used in cool, cold climates. There are also big differences between the people in the models. In the UTCI and PET models, there is a "standardized human" (this human representing a group does not exist in reality), and in the clothing index model, there are individuals. These humans can be characterized in terms of worn or simulated clothing, activity, and thermal perception. In the UTCI and PET models, the thermal insulation value of the clothing is an input variable. In the UTCI model, the thermal insulation of clothing is estimated according to Havenith et al. (2012); in the PET model, its value is 0.9 clo. In the clothing index model, the thermal insulation of clothing is an output variable, which refers to a virtual clothing achieving the thermal equilibrium between the human body and the environment. There are also differences regarding human activity. In the PET model, there is a "standardized human" sitting indoors. In the UTCI and clothing index model, the human walks outdoors at a speed of 1.1 ms^{-1}. Regarding the description of the human thermal

sensation, the differences are very large. In the PET model, there is 9-point thermal sensation scale together with 9-point physiological stress level scale (Matzarakis and Mayer 1996). In the UTCI model, there is no thermal sensation scale at all, a 10-point scale is used for expressing thermal stress intensity (Bröde et al. 2012). In the clothing index model, a 7-point thermal perception scale is used, in which the designation of the categories is very similar to the one used in the ASHRAE 7-point scale (Enescu 2019).

The comparison of thermal loads obtained by different methods is only possible by comparing the thermal perceptions they cause. But a comparison of thermal sensations is difficult if the scales created for their characterization are different. The work of Potchter et al. (2022) deals with the analysis of these difficulties. In biometeorological research, and also in Potchter et al.'s (2022) work, the case of "thermal neutrality" has always been a very popular topic that has received much attention. Since Potchter et al. (2018, 2022) unequivocally showed that the amount of thermal load that characterizes "thermal neutrality" (comfort zone) depends on the type of climate, we will focus only on Köppen's *Cfb* climate type, which is the prevailing climate type in the Hungarian lowland. In the case of "thermal neutrality," PET is between 18 and 23 ℃ according to Matzarakis and Mayer (1996). A somewhat broader PET range (PET between 13 and 22.5 ℃) is obtained by Kovács et al. (2016). In the same case, clothing thermal resistance values change between 0 and 0.5–0.7 clo. The UTCI method uses thermal stress categories, not thermal perception categories. In the UTCI assessment scale, the stress category "no thermal stress" is the closest to "thermal neutrality." During the occurrence of this category, the UTCI values are between 9 and 26 ℃. In our research (Ács et al. 2022), we were also convinced that in this interval of UTCI values, the thermal perception type "cool" was the most common, in addition to the fact that "neutral" and "cold" were also perceived. As we see, it is hard, almost impossible to be very precise in the comparison of different thermal load estimation methods because thermal perception scales also differ significantly. To overcome this difficulty, Potchter et al. (2022) proposes a biometeorological research protocol, where the statistical analysis of the observed data is a decisive methodological element. Note that in our research, data quality control and filtering of thermal load-thermal sensation data were also performed (Section 2.3).

In the science of modelling, it is extremely important to use the simplest models possible. The original r_{cl} model (Ács et al. 2020b) is quite complex, not its human, rather its environmental physics part. The complexity of the environmental physics part can be reduced significantly by a simpler calculation of operative temperature. T_o is well correlated by both PE and T_a. Both relationships have their advantages

and drawbacks. T_o is more similar to PE, than to T_a, since it depends upon radiation, air temperature, and wind speed like PE. However, PE is less usable in cold climates than T_a. Of course, the usage of PE increases the complexity of the model. We investigated both relationships, here only the T_o–PE statistical relationships are used and considered. The statistical approach is used not only for determining T_o but also for establishing the connection between thermal perception type and r_{cl}. By establishing this link, the model is able to estimate not only individual human thermal load but also individual human thermal sensation, which is the ultimate goal of any human climate application. By using this latter statistical part of the model, we avoided the simulation of complex thermoregulation processes, such as sweating, shivering, vasodilation, and vasoconstriction. However, as we mentioned, persons 1 and 2 did not sweat or shiver at all during their observations. We agree with the opinion of Staiger et al. (2019) that human thermoregulation processes need to be simulated for human thermal comfort purposes; nevertheless, in our opinion, this complex model part can be ignored if the goal is to determine individual human thermal climate.

Of course, this first statistical deterministic model aiming at human thermal climate classification also has its drawbacks. Firstly, it is less applicable in warm climates; moreover, it is not applicable at all in the summer season of warm climates. The model would be applicable in the case of simulating the process of sweating. However, in a such model, thermal load is proportional not only to the clothing's thermal resistance but also to the evaporative resistance of the skin (Parsons 2003). Extending the model in this way is one of our future tasks. Secondly, as a statistical model, it has also spatial–temporal limits to its application. Of course, it can be applied under similar geographical conditions, but the T_o–PE connection needs to be recalibrated in regions where annual PE is less than 450 mm•year^{-1} and higher than 750 mm•year^{-1}. The model can also serve for establishing possible human thermal sensation type, especially for humans whose M while walking is around 130–145 Wm^{-2} and when the thermal load is moderate or less. Thermal sensation type is much less estimable with this model in more extreme climates and for humans whose M while walking is substantially different to 130–145 Wm^{-2}. As mentioned, we can talk only about individual human thermal sensation types, but these individual thermal sensation types can be quite similar or even identical if the environmental and human conditions are not extreme.

Since we estimated T_o via PE, r_{cl} is considered for the month of July, the vegetation period, and the year. In the month of July, in lowland and hilly areas, the model was not applicable. As mentioned, the reason is that the energy balance of the human body covered with clothing is not met.

In mountains, besides thermal perception type "neutral," "cool," or even "cold" can also be sensed. These results are in accordance with the results obtained by deterministic models, which are more recent and simpler (Ács et al. 2020b), or more complex and based on a completely different treatment (e.g., Matzarakis and Gulyás 2006; Gulyás and Matzarakis 2009). In the vegetation period, the prevailing human sensation type is "cool." Of course, the largest probability of perceiving thermal type "cold" is in the mountains, where r_{cl} values can reach 1.2 (clo). Regarding annual perceptions, a relief-based configuration emerges. In lowlands, the dominant perception types are both "neutral" and "cool" depending on the person and their psychophysiological state; in hilly areas, it is more only "cool," whilst in mountains, both "cool" and "cold" are common depending on the person and their psychophysiological state. In our treatments, thermal perceptions of persons 1 and 2 are equated with thermal perceptions of a representative Hungarian male and female (persons 3 and 4), respectively. Of course, we did so arbitrarily knowing that the difference between the M values of the persons is less than 15 Wm^{-2}. As we have seen, there is a shift of 0.1–0.2 (clo) in the thermal load between Hungarian males and females. This is caused by the shift in their M values (the M of males is 147, whilst the M of females is 135 Wm^{-2}). However, such a shift in the thermal perceptions between persons 1 and 2 was not registered, which is logical because the difference between their M values is small. It can be said, that sex difference seems to be not a determinant factor in the process of human thermal sensation, especially for moderate or lower thermal loads.

The model presented can be treated as an improved version of Ács et al.'s (2021a) statistical model for estimating r_{cl}, since personal r_{cl} values are simulated and not human groups like, for instance, ectomorphic and/or endomorphic humans. Moreover, here, thermal sensation type estimates are also presented. In summary, this method can be considered as a Feddema (2005) model version, which serves for representing human thermal climate since PE is converted into a personal r_{cl} value, and the personal r_{cl} value into a personal thermal perception type. Of course, Feddema's (2005) "cool" and "cold" categories are not to be confused with the human perception types "cool" and "cold." As we have already seen, Feddema's category "cool" can be perceived either as "neutral or as "cool" or even as "cold" (see thermal sensation of person 2), and similarly, Feddema's category "cold" either as "cold" or as "cool" or even as "very cold" depending on the person and their psychological state. The work of Ács et al. (2021a) showed that human thermal load depends on body shape. If human thermal perception also depended on body shape, it would be much easier to estimate individual human thermal perception categories. Of course, the hypothesis of human thermal perception–body shape link has to be checked, this is a task for the future.

7 Conclusion

The following main conclusions can be drawn: (1) a new statistical deterministic model is presented and validated for estimating human thermal load and sensation for individuals. (2) The model is not applicable in time periods with high thermal load. (3) The results of the model can be used as extra human information in the Feddema (2005) model. (4) The model can be applied outside the region considered, if new region-specific T_o–PE and human-specific thermal sensation-r_{cl} statistical relationships are installed instead of those presented. (5) Human thermal sensation in the Carpathian region is governed by relief. In the Carpathian region's lowland areas, the annual thermal sensation of the vast majority of people is mostly "neutral" or "cool," in mountains mostly "cool" or "cold." (6) There are thermal load differences between the sexes; however, these are not so large that thermal sensation differences between the sexes could be registered.

Data availability CarpatClim dataset is available from the website. Weather and thermal sensation data collected by persons 1 and 2 are available from the corresponding author upon request.

Code availability The code is available from the corresponding author upon request.

Declarations

Ethics approval There was no need to have it.

Consent to participate Consent was obtained from all subjects involved in the study.

Consent for publication Consent for publication was obtained from all authors and subjects involved in the study.

Conflict of interest The authors declare no competing interests.

References

Ács F, Zsákai A, Kristóf E, Szabó AI, Breuer H (2020) Carpathian basin climate according to Köppen and a clothing resistance scheme. Theor Appl Climatol 141:299–307. https://doi.org/10.1007/s00704-020-03199-z

Ács F, Zsákai A, Kristóf E, Szabó AI, Breuer H (2020) Human thermal climate of the Carpathian Basin. Int J Climatol 41(S1):E1846–E1859. https://doi.org/10.1002/joc.6816

Ács F, Kristóf E, Zsákai A, Kelemen B, Szabó Z, Marques Vieira LA (2021) Weather in the Hungarian lowland from the point of view of humans. Atmosphere 12:84. https://doi.org/10.3390/atmos12010084

Ács F, Kristóf E, Zsákai A (2022) Individual local human thermal climates in the Hungarian lowland: estimations by a simple clothing resistance-operative temperature model. Int J Climatol. https://doi.org/10.1002/joc.7910

Ács F, Zsákai A, Kristóf E, Szabó AI, Feddema J, Breuer H (2021a) Clothing resistance and potential evapotranspiration as thermal climate indicators—the example of the Carpathian region. Int J Climatol :1–14. https://doi.org/10.1002/joc.7008

Auliciems A, Kalma JD (1979) A climatic classification of human thermal stress in Australia. J Appl Meteorol 18:616–626

Bašarin B, Kržić A, Lazić L, Lukić T, Đorđević J, JanićijevićPetrović B, Čopić S, Matić D, Hrnjak I, Matzarakis A (2014) Evaluation of bioclimate conditions in two special nature reserves in Vojvodina (Nothern Serbia). Carpathian J Earth Environ Sci 9(4):93–108

Bašarin B, Lukić T, Mesaros M, Pavić D, Đorđević J, Matzarakis A (2018) Spatial and temporal analysis of extreme bioclimate conditions in Vojvodina. Nothern Serbia Int J Climatol 38(1):142–157

Blazejczyk K, Epstein Y, Jendritzky G, Staiger H, Tinz B (2012) Comparison of UTCI to selected thermal indices. Int J Biometeorol 56:515–535. https://doi.org/10.1007/s00484-011-0453-2

Bodzsár É, Fehér VP, Vadászi H, Zsákai A (2016) A női nemi hormonok szintje és a testzsírosság kapcsolata pubertáskorú leányoknál (Sex hormonal levels and body fatness in pubertal girls). Anthropológiai Közlemények 57, 51–60 (in Hungarian)

Bröde P, Fiala D, Blazejczyk K, Holmér I, Jendritzky G, Kampmann B, Tinz B, Havenith G (2012) Deriving the operational procedure for the universal thermal climate index (UTCI) Int J Biometeorol 56(3):481–494

Campbell GS, Norman JM (1998) An introduction to environmental biophysics, 2nd edn. Springer, New York, 286 pp

Cheval S, Birsan M-V, Dumitrescu A (2014) Climate variability in the Carpathian mountains region over 1961–2010. Glob Planet Change 118:85–96. https://doi.org/10.1016/j.gloplacha.2014.04.005

de Freitas CR, Grigorieva EA (2015) A comprehensive catalogue and classification of human thermal climate indices. Int J Biometeorol 59:109–120

Dubois D, Dubois EF (1915) The measurement of the surface area of man. Arch Intern Med 15:868–881. https://doi.org/10.1001/archinte.1915.00070240077005

Enescu D (2019) Models and indicators to assess thermal sensation under steady-state and transient conditions. Energies. 12(5):841. https://doi.org/10.3390/en12050841

Fanger PO (1973) Assessment of man's thermal comfort in practice. Br J Ind Med 30:313–324

Fanger PO (1970) Thermal comfort: analysis and applications in environmental engineering. PhD Thesis, Danmarks tekniske højskole,

Danish Technical Press, Copenhagen, 244 pp. ISBN: 8757103410 9788757103410.

Feddema JJ (2005) A revised Thornthwaite-type global climate classification. Phys Geogr 26:442–466

Fiala D, Havenith G, Bröde P, Kampmann B, Jendritzky G (2011) UTCI-Fiala multi-node model of human heat transfer and temperature regulation. Int J Biometeorol 56(3):1–13

Gagge AP, Fobelets AP, Berglund LG (1986) A standard predictive index of human response of the thermal environment. ASHRAE Trans 92:709–731

Gulyás Á, Matzarakis A (2009) Seasonal and spatial distribution of physiologically equivalent temperature (PET) index in Hungary. Időjárás 113(3):221–231

Gulyás Á, Unger J, Matzarakis A (2006) Assessment of the microclimatic and human comfort conditions in a complex urban environment: modelling and measurements. Build Environ 41:1713–1722

Hantel H, Haimberger L (2016) Grundkurs Klima. Springer Spektrum, Berlin, Heidelberg, 404 pp. https://doi.org/10.1007/978-3-662-48193-6

Havenith G, Fiala D, Blazejczyk K, Richards M, Bröde P, Holmér I, Rintamaki H, Benshabat Y, Jendritzky G (2012) The UTCI-clothing model. Int J Biometeorol 56(3):461–470

von Humboldt A (1845) Kosmos: Entwurf einer physischen Weltbeschreibung (Cosmos: a sketch of the physical description of the Universe), Cotta, Tübingen (in German).

Jendritzky G, de Dear R, Havenith D (2012) UTCI–why another thermal index? Int J Biometeorol 56:421–428

Kántor N, Égerházi L, Unger J (2012) Subjective estimation of thermal environment in recreational urban spaces-Part 1: investigation in Szeged. Int J Biometeorol 56:1075–1088

Köppen W (1936) The geographic system of climates (original: Das geographische System der Klimate). In: Köppen W and Geiger R (eds) Handbuch der Klimatologie, Bd. 1, Teil C, Borntraeger, Berlin, 44 pp.

Kovács A, Németh Á (2012) Tendencies and differences in human thermal comfort in distinct urban areas in Budapest, Hungary. Acta Climatol Chorol Univ Szegediensis 46:115–124

Kovács A, Unger J (2013) Modification of the tourism climatic index to Central European climatic conditions–examples. Időjárás 118(2):147–166

Kovács A, Unger J, Gál C, Kántor N (2016) Adjustment of the thermal component of two tourism climarological assessment tools using thermal perception and preference surveys from Hungary. Theor Appl Climatol 125:113–130. https://doi.org/10.1007/s00704-015-1488-9

Lakatos M, Szentimrey T, Bihari Z, Szalai S (2013) Creation of a homogenized climate database for the Carpathian region by applying the MASH procedure and the preliminary analysis of the data. Időjárás 117(1):143–158

Matzarakis A (2020) A note on the assessment of the effect of atmospheric factors and components on humans. Atmosphere 11:1283. https://doi.org/10.3390/atmos11121283

Matzarakis A, Gulyás Á (2006) A contribution to the thermal bioclimate of Hungary–mapping of the physiologically equivalent temperature. In: Kiss A, Mezősi G, Sümeghy Z (eds) Landscape, Environment and Society. Studies in Honour of Professor Ilona Bárány-Kevei on the Ocassion of Her Birthday. University of Szeged, pp 479–488

Matzarakis A, Mayer H (1996) Human-biometeorologische Untersuchungen in den höheren Lagen des Schwarzwaldes. Proceedings of the 24th International Conference on Alpine Meteorology, Ljubljana, pp 417–423

Mayer H, Höppe P (1987) Thermal comfort of man in different urban environments. Theor Appl Climatol 38:43–49

McKenney MS, Rosenberg NJ (1993) Sensitivity of some potential evapotranspiration methods to climate change. Agric for Meteorol 64:81–110. https://doi.org/10.1016/0168-1923(93)90095-Y

Mifflin MD, St Jeor ST, Hill LA, Scott BJ, Daugherty SA, Koh YO (1990) A new predictive equation for resting energy expenditure in healthy individuals. Am J Clin Nutr 51:241–247. https://doi.org/10.1093/ajcn/51.2.241.DOI:10.1093/ajcn/51.2.241

Németh Á (2011) Changing thermal bioclimate in some Hungarian cities. Acta Climatol Chorol Univ Szegediensis 44–45:93–101

Parsons KC (2003): Human thermal environments, 2nd edn. Taylor & Francis, London and New York, 538 pp

Potchter O, Cohen P, Lin TP, Matzarakis A (2018) Outdoor human thermal perception in various climates: a comprehensive review of approaches, methods and quantification. Sci Total Environ. https://doi.org/10.1016/j.scitotenv.2018.02.276

Potchter O, Cohen P, Lin TP, Matzarakis A (2022) A systematic review advocating a framework and benchmarks for assessing outdoor human thermal perception. Sci Total Environ. https://doi.org/10.1016/j.scitotenv.2022.155128

Staiger H, Laschewski G, Graetz A (2012) The perceived temperature – a versatile index for the assessment of the human thermal environment. Part A: scientific basics. Int J Biometeorol 56:165–176

Staiger H, Laschewski G, Matzarakis A (2019) Selection of appropriate thermal indices for applications in human biometeorological studies. Atmosphere 10:18. https://doi.org/10.3390/atmos10010018

Szentimrey T, Bihari Z (2013) Meteorological interpolation based on surface homogenized data basis (MISH v1.02). In: Bihari Z (ed) CARPATCLIM, Climate of the Carpathian Region, Deliverable D2.10, Final version of metadata per country of all national gridded datasets created within module 2. Annex 3 – Description of MASH and MISH algorithms, 100 pp. http://www.carpatclim-eu.org/pages/deliverables/

Szentimrey T (1999) Multiple analysis of series for homogenization (MASH). Proceedings of the Second Seminar for Homogenisation of Surface Climatlogical Data, Budapest, Hungary; WMO, WCDMP-No. 41, 27–46.

Thornthwaite CW (1948) An approach toward a rational classification of climate. Geogr Rev 38:55–94. https://doi.org/10.2307/210739

Weyand PG, Smith BR, Puyau MR, Butte NF (2010) The mass-specific energy cost of human walking is set by stature. J Exp Biol 213:3972–3979. https://doi.org/10.1242/jeb.048199

Zhao Q, Lian Z, Lai D (2021) Thermal comfort models and their developments: a review. Energy and Built Environment (EBE) 2:21–33

Zsákai A, Mascie-Taylor N, Bodzsár ÉB (2015) Relationship between some indicators of reproductive history, body fatness and the menopausal transition in Hungarian women. J Physiol Anthropol 34(1):35–42. https://doi.org/10.1186/s40101-015-0076-0